# Dynamics and Control of Single-Line Kites

**Article** *in* Aeronautical Journal -New Series- · September 2006

DOI: 10.1017/S0001924000001470

CITATIONS
28

READS
1,548

**1 author:**

Gonzalo Sanchez-Arriaga
University Carlos III de Madrid
**141** PUBLICATIONS **1,066** CITATIONS

SEE PROFILE

# Dynamics and control of single-line kites

**G. Sánchez**
Dept Física Aplicada, ETSI Aeronáuticos,
Universidad Politécnica,
Madrid, Spain

## ABSTRACT

This paper presents a dynamic analysis of a single-line kite with two degrees of freedom. A Lagrangian formulation is used to write convenient equations of motion. The equilibrium states of the system and their stability are studied; Eigenvalues and eigenmodes are calculated by using linear theory. The stability in the parametric plane $\delta - W_0$ is discussed, where $\delta$ defines the bridle geometry and $W_0$ is wind velocity. The system goes through a Hopf bifurcation and periodic branches of solutions appear. The orbits and their stability have been calculated numerically using Floquet theory and wind velocity seems to play an important role in their existence. Finally the kite response against gusts is considered and an open loop control system developed to keep the flight altitude invariant under changing atmospheric conditions. Modifying the bridle's geometry seems to be a convenient way to control a kite's performance.

## NOMENCLATURE

| | |
|---|---|
| $A$ | kite's area (m$^2$) |
| $c$ | kite's chord (m) |
| $C_N$ | aerodynamic normal force coefficient |
| $g$ | acceleration due to gravity (ms$^{-2}$) |
| $h_0$ | altitude of the kite (m) |
| $l$ | length of the line (m) |
| $m$ | kite's mass (kg) |
| $I_y = mr_g^2$ | moment of inertia about $y$ axis (kgm$^2$) |
| $r$ | bridle length in Fig. 1 (m) |
| $r_g$ | radius of gyration (m) |
| $T$ | period (s) |
| $T_{1/2} = -Ln2/\eta$ | damping time (s) |
| $\mathbf{V_A}$ | kite aerodynamic velocity (ms$^{-1}$) |
| $\mathbf{W_0}$ | wind velocity (ms$^{-1}$) |
| $\mathbf{X}$ | state vector |
| $x_{COP}$ | distance to centre of pressure from leading edge (m) |
| $x_G$ | distance to centre of mass from leading edge (m) |
| $x_{CP}$ | distance to centre of mass from centre of pressure(m) |
| $\alpha$ | angle of attack (deg) |
| $\alpha_s$ | stall angle (deg) |
| $\delta$ | bridle angle in Fig. 1 (deg) |
| $\Gamma$ | azimuth angle of the line at the ground (deg) |
| $\eta$ | real part of $\nu$ ($s^{-1}$) |
| $\nu$ | stability root |
| $\rho$ | air density (kg/m$^3$) |
| $\theta$ | pitch Angle (deg) |
| $\omega$ | imaginary part of $\nu$ (rad/s$^{-1}$) |

### Subscripts

| | |
|---|---|
| $B$ | body system |
| $T$ | earth system |
| $G$ | term pertaining to the mass center |

## 1.0 INTRODUCTION

Kites are the oldest flying machines and their charm fascinates people of every age. They contributed to aeronautical development but, after the first flights, airplanes became the centre of attention and kites were relegated to be a child's toy. However, there are exceptions that will now be recalled.

The earliest research into kites appears in England during WW1. Glauert[1] and Bairstow[2] used simplified models to demonstrate the possibility of system instability. In 1942 L.W. Bryant, W.S. Brown and

**Paper No. 3048**. Manuscript received 13 December 2005, revised version received 9 January 2006, accepted 27 March 2006.

N.E. Sweeting[3] studied the kite problem with the object of settling whether or not it was possible to make a stable kite with a high lift/drag ratio. They found that the presence of the cable has the effect of raising the degree of the stability equations, introducing new modes of oscillation not possible in free airplanes. In general, the original modes of motion remain stable but modified in amplitude and period, however new unstable modes appears.

R.A. Adomaitis[4] formulated a simplified model of one degree of freedom for kite flight. He proved the possibility of multiple equilibrium states and the existence of a bifurcation point (Hopf) in the wind velocity/kite-string angle plane. In his model, the angle between the principal line and the kite was considered as constant and this constraint allowed him to find analytical results. This last assumption is not considered in present model, leading to a system with two degrees of freedom.

Later, K. Alexander and J. Stevenson[5] studied the influence of the kite bridle and verified the existence of multiple equilibrium states. In their experiments, they found that for each wind speed, a particular bridle geometry is required in order to reach the optimum ratio between kite lift and drag. This idea will be used here to control the altitude of the kite under non stationary atmospheric conditions.

The impact of the bridle configuration on the structure of the kite was investigated by S.L. Veldman *et al*[6] which provided numerical results allowing to find the optimum material for the principal line. This issue has a major impact on the performance of the whole system and this structural design concept has been proposed in order to break the world altitude record for kites.

The nonlinear model predictive controller (NMPC) for periodic unstable systems formulated by M. Diehl *et al*[7] was used to a dual line kite. This NMPC controller makes use of a target function and an additional constraint equation which avoids that the kite hits the ground. In consequence, the motion is controlled in a plane in front of the kite flier instead of our model where the control takes place in a vertical plane.

In the present paper the physical model for the dynamics of tethered aerostats introduced by J. DeLaurier[8], is used to investigate the dynamics and control of single-line kites. In this formulation the presence of the tension force leads to a difficult mathematical problem. As we shall see, the Lagrangian formulation simplifies the equations when the connection between the bridle and principal line is considered as an ideal, non dissipative union. In this case, the tension force does not appear in the model because in any virtual displacement allowed by the constraints the tension does no work.

This article is organised as follows. In Section 2 the physical model is formulated as well as the kite equations of motion. The system could have multiple equilibrium states in particular for low attack angles. This equilibrium is discussed in Section 3, the influence of the parameter δ (bridle geometry) and the effect of wind velocity. The linear stability of the kite and the eigenmodes are analysed in Section 4. The periodic orbits and their stability are numerically calculated in Section 5. An open loop control system shows how by changing bridle geometry the kite flight altitude can be controlled even under non stationary atmospheric conditions in Section 6. Finally, we end with some concluding remarks.

## 2.0 EQUATIONS OF MOTION

### 2.1 Lagrangian function

The system is a tethered body immersed in a homogeneous fluid stream and it can be divided into three parts: the kite, the bridle and the principal line. The equations will be derived with the following assumptions[8]:

- The kite is a rigid and symmetric body. The aerodynamic characteristics will be calculated using a flat plate model[9] (see Fig. 2).

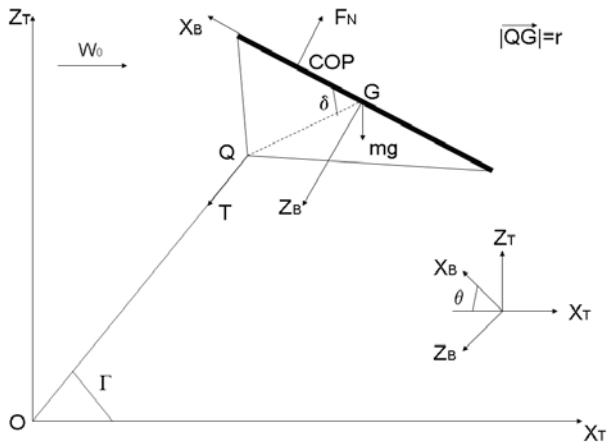


Figure 1. Generalised co-ordinates.

- The bridle lines are always under traction forces and they can be considered rigid solids.
- The principal line may be dynamically considered to be a massless, dragless rigid rod with frictionless pivots at the ground attachment and the confluence point $Q$, see Fig 1.

The cable lies in a vertical plane that bisects the kite. Figure 1 shows that the co-ordinate system used $(x, y, z)_T$ is an inertial frame while $(x, y, z)_B$ is a non inertial body fixed frame attached to the kite with origin at its centre of mass and moving with it. The body axes are the principal axes of the kite. Only the longitudinal dynamics will be considered and lateral movements will be neglected.

A rigid body, free from constraints, has six independent co-ordinates or degrees of freedom. In the actual model the kite is constrained to move in a vertical plane so it has only three degrees of freedom, for instance the mass centre co-ordinates $(x_G, 0, z_G)$ and the pitch angle θ. However, the principal line and the bridle impose an additional holonomic constraint $f(x_G, z_G, \theta, t) = 0$ that limit the motion of the system. Therefore the system has only two degrees of freedom.

Constraints introduce two types of difficulties in the solution of mechanical problems. First the co-ordinates are no longer all independent and second the force of constraint (the tension force in the kite problem) is not furnished a priori. In the case of holonomic constraints the first difficulty is removed by the introduction of generalised co-ordinates. These co-ordinates in the present system will be the pitch angle of the kite θ and the azimuth angle of the principal line Γ, see Fig. 1. The second difficulty is solved if the constraints are workless in a virtual displacement. In this case the constraint forces do not appear in the equations.

Two parameters, δ and $r$, define the bridle's geometry and they will be considered known functions of time. They will be used as the control parameter in Section 6. If the kite is without control, that is $dr/dt = d\delta/dt = 0$, the constraint equation reads as $f(x_G, z_G, \theta) = 0$ and the system is holonomic and scleronomous. However, if the control is activated, $dr/dt \neq 0$ or $d\delta/dt \neq 0$, then $f(x_G, z_G, \theta, t) = 0$ and the system is holonomic and rheonomous.

For writing down the Lagrangian function of the system some previous calculation must be done. Using the generalised co-ordinates the mass centre position of the kite is

$$\mathbf{r_G} = \begin{pmatrix} x_G \\ y_G \\ z_G \end{pmatrix}_T = \begin{pmatrix} l\mathrm{Cos}\Gamma + r\mathrm{Cos}(\delta - \theta) \\ 0 \\ l\mathrm{Sin}\Gamma + r\mathrm{Sin}(\delta - \theta) \end{pmatrix}_T \qquad \ldots (1)$$

Now the velocity vector reads

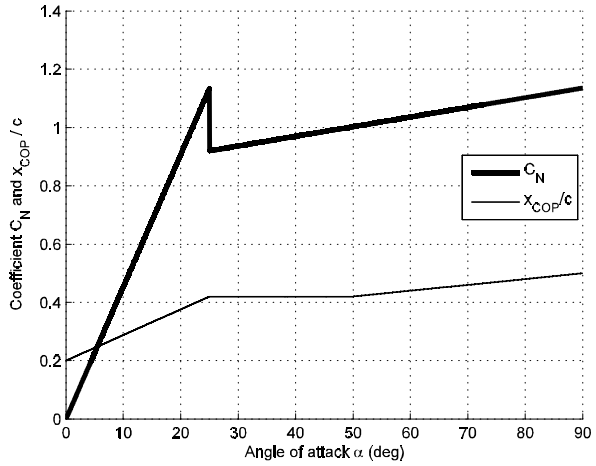


Figure 2. Normal force coefficient and centre of pressure position.

$$\mathbf{v_G} = \begin{pmatrix} \dot{x}_G \\ \dot{y}_G \\ \dot{z}_G \end{pmatrix}_T = \begin{pmatrix} -l\dot{\Gamma}\,\mathrm{Sin}\Gamma + \dot{r}\,\mathrm{Cos}(\delta-\theta) - r\,\mathrm{Sin}(\delta-\theta)(\dot{\delta}-\dot{\theta}) \\ 0 \\ l\dot{\Gamma}\,\mathrm{Cos}\Gamma + \dot{r}\,\mathrm{Sin}(\delta-\theta) + r\,\mathrm{Cos}(\delta-\theta)(\dot{\delta}-\dot{\theta}) \end{pmatrix}_T \quad \ldots(2)$$

and the angular velocity of the solid becomes

$$\boldsymbol{\omega} = \dot{\theta}\,\mathbf{j}_{\delta} \quad \ldots(3)$$

Following the usual procedure, the kinetic and potential energies of the system are respectively:

$$T = \frac{1}{2}mV_G^2 + \frac{1}{2}I_y\dot{\theta}^2 \quad \ldots(4)$$

$$V = mgz_G \quad \ldots(5)$$

The Lagrangian function $L$ can be calculated as:

$$L = T - V = f(\dot{\Gamma},\Gamma,\dot{\theta},\theta,t) \quad \ldots(6)$$

## 2.2 Generalised forces

Since the tension of the line does no work and the weight of the kite is potential energy, only aerodynamic forces need to be considered. Normal aerodynamic force and moment can be expressed as

$$\mathbf{F_A} = -\frac{1}{2}\rho AV_A^2 C_N \mathbf{k_B} \quad \ldots(7)$$

$$\mathbf{M_A} = \frac{1}{2}\rho AV_A^2 C_N x_{CP}\mathbf{j_B} \quad \ldots(8)$$

where:

$$\mathbf{V_A} = \mathbf{V_G} - W_0\mathbf{i_T} \quad \ldots(9)$$

$$x_{cp} = (x_G - x_{COP}) \quad \ldots(10)$$

The normal force coefficient, $C_N$, and the dimensionless center of pressure position $x_{COP}/c$ are dependent on the attack angle α and they are shown in Fig. 2. The attack angle can be calculated using:

$$\alpha = \theta + \mathrm{ATan}\left(\frac{\mathbf{V_A}\cdot\mathbf{k_T}}{\mathbf{V_A}\cdot\mathbf{i_T}}\right) \quad \ldots(11)$$

The terms that must be added to the Lagrange equations due to the aerodynamic forces are:

$$Q_\Gamma = \mathbf{F_A}\cdot\frac{\partial\mathbf{V_G}}{\partial\dot{\Gamma}} + \mathbf{M_A}\cdot\frac{\partial\omega}{\partial\dot{\Gamma}} = \frac{1}{2}\rho AV_A^2 C_N l\,\mathrm{Cos}(\Gamma+\theta) \quad \ldots(12)$$

$$Q_\theta = \mathbf{F_A}\cdot\frac{\partial\mathbf{V_G}}{\partial\dot{\theta}} + \mathbf{M_A}\cdot\frac{\partial\omega}{\partial\dot{\theta}} = \frac{1}{2}\rho AV_A^2 C_N\left(x_{cp} - r\,\mathrm{Cos}\delta\right) \quad \ldots(13)$$

## 2.3 Lagrange's equations

Once the Lagrangian function and the terms due to the aerodynamic forces are calculated, the equations of motion can be written down,

$$\frac{\mathrm{d}}{\mathrm{d}t}\left(\frac{\partial L}{\partial\dot{\Gamma}}\right) - \frac{\partial L}{\partial\Gamma} = Q_\Gamma \quad \ldots(14)$$

$$\frac{\mathrm{d}}{\mathrm{d}t}\left(\frac{\partial L}{\partial\dot{\theta}}\right) - \frac{\partial L}{\partial\theta} = Q_\theta \quad \ldots(15)$$

In order to simplify the notation, the following auxiliary functions will be used:

$$f_1 = \mathrm{Sin}(\delta-\theta-\Gamma) \quad f_2 = \mathrm{Cos}(\delta-\theta-\Gamma) \quad \hat{r}(t) = \frac{r}{l}$$
$$\hat{x}_{CP} = \frac{x_{CP}}{l} \qquad \hat{V}_A = \frac{V_A}{\sqrt{gl}} \quad \ldots(16)$$

the dimensionless parameters:

$$\hat{r}_g = \frac{r_g}{l} \qquad \mu = \frac{\rho Al}{2m} \quad \ldots(17)$$

and a dimensionless time $\tau = \sqrt{\frac{g}{l}}t$. A state vector $\mathbf{x} = \left(\dot{\Gamma},\Gamma,\dot{\theta},\theta\right)$ is introduced and using these variables, our equations read:

$$\frac{\mathrm{d}\boldsymbol{x}}{\mathrm{d}\tau} = \boldsymbol{h}_i(\boldsymbol{x},t) \quad \ldots(18)$$

where

$$\mathbf{h_1} = \begin{pmatrix} \frac{1}{|A|}\left[\left(\hat{r}_g^2 + \hat{r}^2\right)g_1 + \hat{r}\,f_2 g_2\right] \\ \dot{\Gamma} \\ \frac{1}{|A|}\left[\hat{r}\,f_2 g_1 + g_2\right] \\ \dot{\theta} \end{pmatrix} \quad \ldots(19)$$

and

$$|A| = \hat{r}_g^2 + \hat{r}^2 f_1^2 \quad \ldots(20)$$

$$g_1 = -\hat{r}\ddot{\delta}\,f_2 - \ddot{\hat{r}}\,f_1 - 2\left(\dot{\delta}-\dot{\theta}\right)\dot{\hat{r}}\,f_2 + \hat{r}\left(\dot{\delta}-\dot{\theta}\right)^2 f_1 \cdot$$
$$-\mathrm{Cos}\Gamma + \mu\hat{V}_A^2 C_N\mathrm{Cos}(\Gamma+\theta) \quad \ldots(21)$$

$$g_2 = 2\dot{\hat{r}}\hat{r}\left(\dot{\delta}-\dot{\theta}\right) + \hat{r}\dot{\Gamma}^2 f_1 + \hat{r}^2\ddot{\delta}\cdot$$
$$+\hat{r}\,\mathrm{Cos}(\delta-\theta) + \mu\hat{V}_A^2 C_N(\hat{x}_{CP} - \hat{r}\,\mathrm{Cos}\delta) \quad \ldots(22)$$

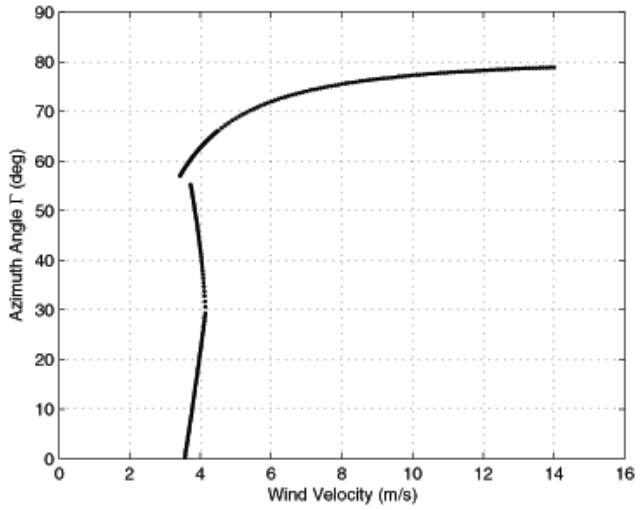


Figure 3. Azimuth angle Γ versus wind velocity.

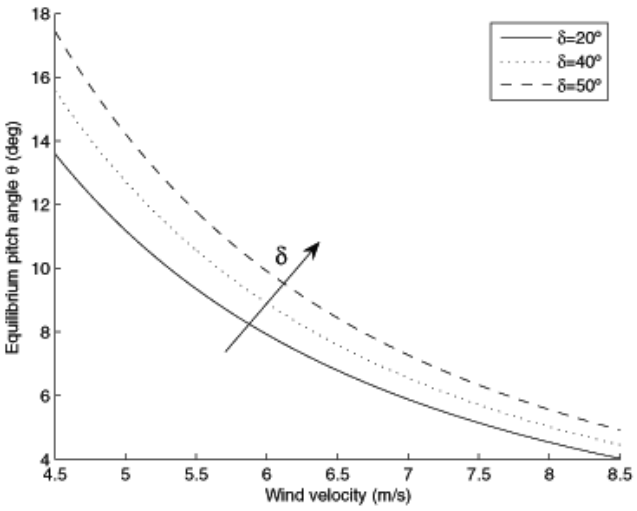


Figure 4. Equilibrium pitch angle versus wind velocity.

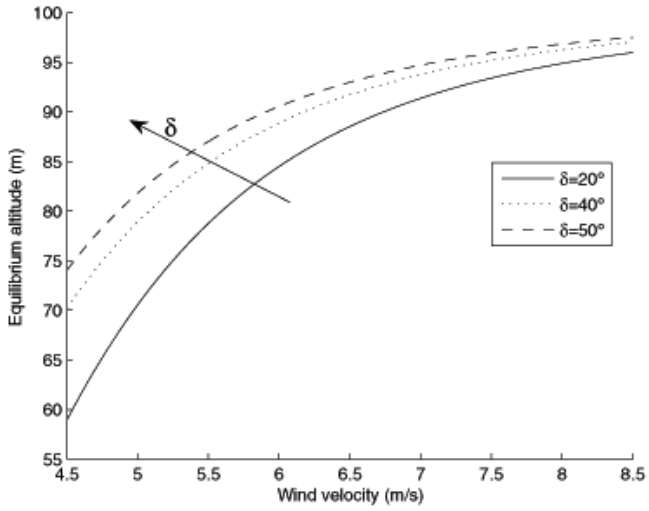


Figure 5. Equilibrium altitude versus wind velocity.

## 3.0 EQUILIBRIUM STATES

Let us assume that the kite is without control, that is $dr/dt = d\delta/dt = 0$. In that case the equations that govern the equilibrium of the system are:

$$\mathrm{Cos}(\delta-\theta)+\beta\left(\sigma-\mathrm{Cos}\delta\right)C_N(\theta)=0 \qquad \ldots (23)$$

$$\Gamma=\mathrm{ATan}\left(\frac{\beta C_N(\theta)\mathrm{Cos}\theta-1}{\beta C_N(\theta)\mathrm{Sin}\theta}\right) \qquad \ldots (24)$$

where:

$$\beta=\frac{\rho A W_0^2}{2mg} \qquad \sigma=\frac{x_{CP}}{r} \qquad \ldots (25)$$

These equations are decoupled. Equation (23) gives the equilibrium pitch angle θ and Equation (24) can be used to calculate Γ afterwards. The equilibrium of the system depends on three aspects: (1) the angle δ, (2) σ, fraction between the moment arm length $x_{cp}$ and the bridle length $r$ and (3) $\beta C_N$ that relates the aerodynamic force and the weight of the kite. Therefore there are two ways to control the kite's equilibrium. The first way, used in the present article, is to modify the geometry of the bridle during the flight ($r$ or δ). The second way is to change the aerodynamic characteristics using a variable $C_N$ or $x_{cp}$.

K. Alexander and J. Stevenson[5] presented a theoretical model and verified experimentally the existence of three equilibrium states of which some could have an attack angle above the stall. In that article (Fig. 9) they calculated the azimuth angle Γ *versus* the wind velocity with a kite of 6kg, 27m², front bridle fixed at 0·75$c$ and aft bridle fixed at 1.0$c$. This bridle correspond to $r$ = 0·7289m and δ = 72·535°. The position of the centre of mass is inferred to be $x_{COM}$ = 0·5$c$. Figure 3 shows the same variables but now using Equations 23 and 24 and the results are in agreement.

In this the paper, we will consider states with $\alpha < \alpha_s$; that is, the normal attitude of the kite during the flight and we will refer to this solution as point $P$. Figures 4 and 5 show solutions of Equations 23 and 24 with typical values for the parameters (see Table 1) . It can be seen how the equilibrium pitch angle decreases and the altitude increases when the wind becomes stronger. Higher wind velocities make the kite fly at a lower angle-of-attack and also with a higher aerodynamic efficiency. Consequently the altitude is greater[3].

## 4.0 STABILITY

The kite's stability can be explored using linear theory: Eigenvalues' real part of the Jacobian matrix gives the stability of fixed points. Let us consider typical values for the parameters (see Table 1) with δ = 45° and $W_0$ = 6ms⁻¹. The state vector **x** has four variables, therefore the characteristic equation has four roots. In the case selected there are

**Table 1**
**Numerical values of the parameters**

| Parameter | Value |
|---|---|
| $m$ | 0·3kg |
| $c$ | 0·8m |
| $S$ | 0·48m² |
| $r_g$ | 0·19m |
| $r$ | 1m |
| $L$ | 100m |
| $x_{COM}$ | 0·4m |
| ρ | 1·225kg/m³ |
| g | 9·8ms⁻² |

**Table 2**
**Mode 1: Pitch mode**

| Characteristic | Value |
|---|---|
| $\eta$ | $-5{\cdot}02 s^{-1}$ |
| $\varpi$ | 10·82rad/s |
| $T_{1/2}$ | 0·14s |
| $T$ | 0·58s |

**Table 3**
**Mode 2: Pendulum mode**

| Characteristic | Value |
|---|---|
| $\eta$ | $-0{\cdot}16 s^{-1}$ |
| $\varpi$ | 0·22rad/s |
| $T_{1/2}$ | 4·22s |
| $T$ | 29·2s |

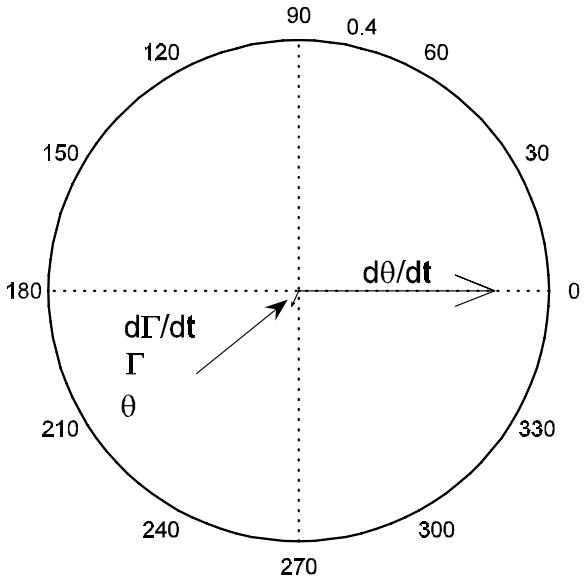


Figure 6. Vector diagram of pitch mode.

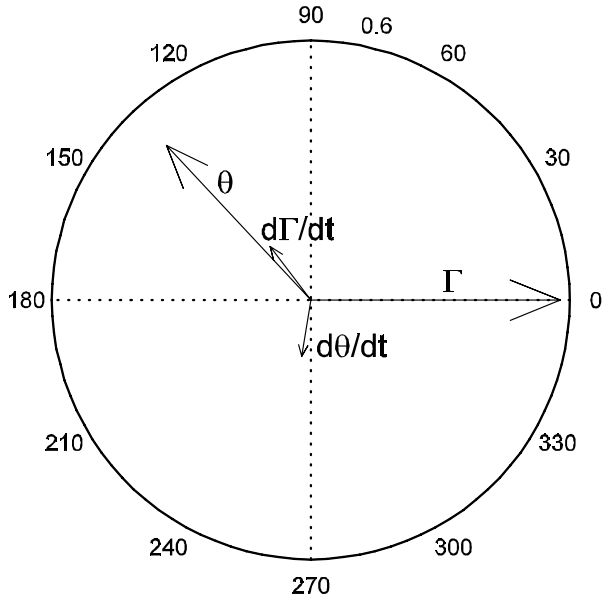


Figure 7. Vector diagram of pendulum mode.

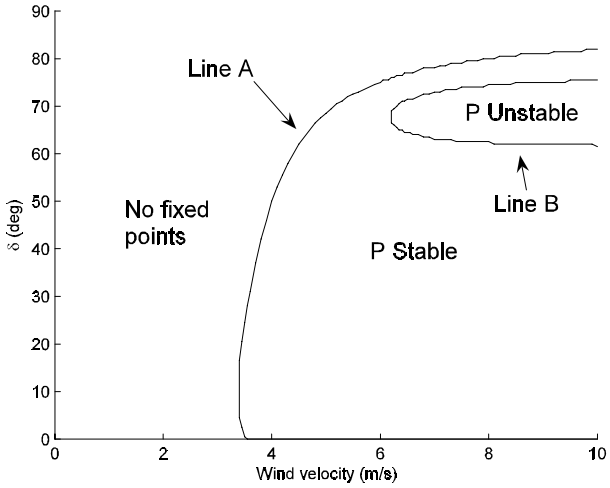


Figure 8. Parametric domain of stability.

two pairs of complex conjugate Eigenvalues, $\nu = \eta \pm i\omega$, and two different Eigenmodes exist. These modes are usually called[8] 'pitch mode' and 'pendulum mode'.

Tables 2 and 3 show the principal characteristic of the eigenmodes. In this case all the Eigenmodes are stable due to the real part of the eigenvalues being negative. Pitch mode has a very high damping and a short period. The angle $\Gamma$ is not excited (the principal line of the kite is calm) and the kite makes a fast movement around point $Q$ (see Fig. 1). Pendulum mode is completely different. The damping is small and the period of the motion is long (~ 29s). Now the angle $\Gamma$ is excited and the kite makes a motion similar to a pendulum. Vector diagrams of both modes are in Figs 6 and 7.

Finally, the stability of the kite can be obtained in the parametric plane $\delta - W_0$ (see Fig. 8). First of all it can be seen how, for each value of $\delta$, a minimum wind velocity exists. Line A separates the regions where the wind velocity is too low to support the kite. The second conclusion is that there exists a region of instability when the control parameter $\delta$ is above 55º. It must be said that probably the stability is underestimated. Dragging along the line has been neglected and the aerodynamic model of the kite underestimates the drag force too. Previous works[3] assert that the stability of the system is improved when the drag is increased in spite of the flight altitude being damaged.

According to the previous paragraph the parameter domain where the kite is stable is quite extensive. This result allows us to develop an open loop control system in order to keep the flight altitude constant.

## 5.0 PERIODIC ORBITS

The numerical explorations carried out show that the eigenvalue that loses stability is complex. Point P goes through a Hopf bifurcation when crossing line B and a branch of periodic solutions is formed. This result was found by R. Adomaitis[4] using a model with one degree of freedom.

However the existence of periodic solutions is not guarantee for the model of the present paper. One requirement of the Hopf bifurcation theorem is that the vector field $\mathbf{h}_1$ must be continuous and the actual model is discontinuous due to the stall of the kite. As a consequence the

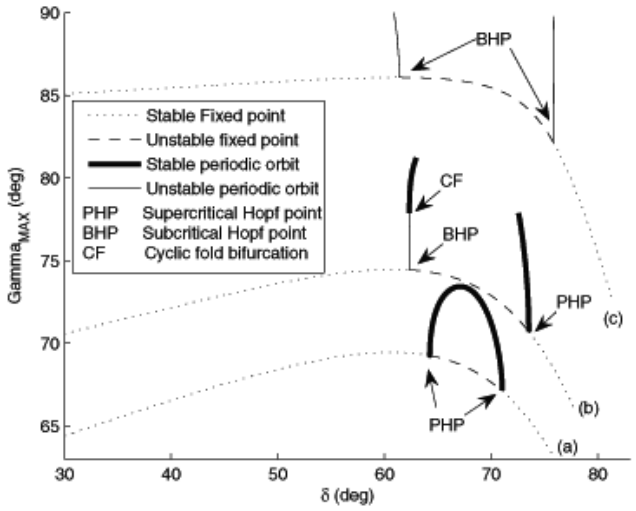


Figure 9. Bifurcation diagram. (a) $W_0$ = 6·5ms$^{-1}$, (b) $W_0$ = 7·5ms$^{-1}$ and (c) $W_0$ = 10ms$^{-1}$.

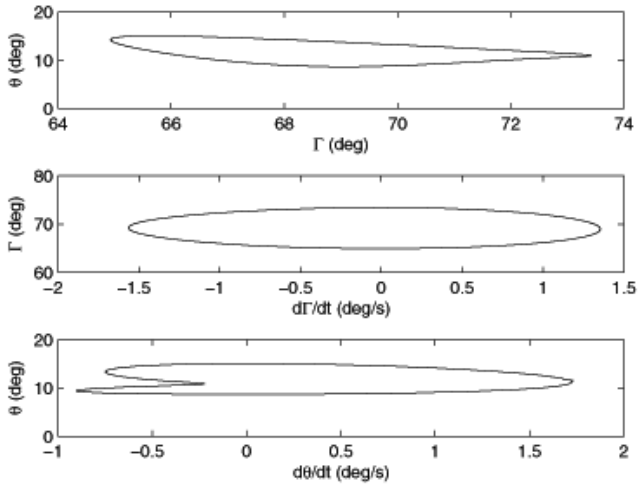


Figure10. Periodic orbit. δ = 67º and $W_0$ = 6·5ms$^{-1}$.

parametric domain in the plane δ – $W_0$ where periodic solutions exist is reduced. To avoid the problem of the stall during the integration of the equations the next procedure has been followed. First a new vector field, $\mathbf{h_2}$, is defined. $\mathbf{h_2}$ is the same as $\mathbf{h_1}$ except (see Fig. 2):

$$C_N = C_{N\alpha}\alpha \qquad \forall\alpha \qquad \ldots (26)$$

With this continuous vector field we present the results of a numerical investigation using a combination of AUTO[10] and XPPAUT[11]. The second step is to check if $\alpha < \alpha_s$ during the orbit. If this condition is true this orbit is a real solution of the system in Equation (18). AUTO allows to track fixed points, find turning points and Hopf bifurcation points and compute branches of periodic solutions emanating from a Hopf point.

Figure 9 shows a bifurcation diagram of the system. $\Gamma_{MAX}$ is the maximum azimuth angle reached during a periodic orbit if the branch is periodic and the solution of Equation (24) if it is a fixed point branch. The angle δ is varied in a broad range and the calculus is done for three different wind velocities: 6·5, 7·5 and 10ms$^{-1}$.

Diagram (a) points out how as δ is increased, the fixed point *P* changes its stability through a supercritical Hopf bifurcation where a branch of periodic solutions is formed. This branch finishes in a second supercritical Hopf bifurcation and *P* changes its stability again (see Figs 8 and 9). Diagram (b) corresponds to a wind velocity of 7·5ms$^{-1}$ and present meaningful differences: now the first Hopf bifurcation is subcritical and the second one remains supercritical. Furthermore the unstable periodic branch experiences a cyclic fold bifurcation (a Floquet multiplier leaves the unit circle through +1) and become stable. Both branches finish because the kite stalls.

When the wind velocity is increased (diagram c) both Hopf bifurcations become subcritical and no stable periodic orbits exist. Now the periodic branches finish because the azimuth angle Γ reaches 90º and in this situation the model is invalid (the principal line is not under traction).

Figure 10 shows projections of the phase space for a particular periodic solution: $W_0$ = 6·5ms$^{-1}$ and δ = 67º. It can be seen how the orbit has a part where Γ increases (kite rising) while the pitch angle decreases and other part where this situation is reversed.

## 6.0 CONTROL SYSTEM

The next section introduces an open loop control system to keep the flight altitude of the kite constant. Traditionally the kite flier makes this operation by changing the length of the principal line because they can wind up or release the line. Note that the present physical model cannot reproduce this operation because the parameter *l* has been assumed constant.

The equations of motion were derived, assuming that both *r* and δ were temporal functions. The combination of both parameters could make the control more robust and powerful. However during the following analysis *r* will be considered constant in order to simplify the problem.

The control system will need to know the wind's velocity and bridle's geometry at each moment and a suitable mechanism to change δ must be on board. The kite may carry an anemometer and an electric motor with a coil to change δ. Varying δ keeping *r* constant could be difficult but it will be assumed that an adequate mechanism exists. Another issue that must be discussed is how to keep bridle line under traction (compressive forces would make the bridle collapse) while δ changes. Again this problem can be solved with a more complicated mechanism that would vary the attachment points between the bridle's lines and the kite.

All these technical problems will be ignored during the following sections. To sum up, only δ will be a temporal function, *r* will be constant and the bridle will have a rigid solid behaviour.

The control law will be the following. The control system will know the altitude, $h_0$, the kite must reach. With this, the angle Γ can be estimated using:

$$\Gamma = \mathrm{ASin}\left(\frac{h_0}{l}\right) \qquad \ldots (27)$$

Then using Equation (24), θ can be obtained and finally with 23 δ. This angle must be imposed by the control and if the system is stable the required altitude will be reached.

In order to present the above control system the behaviour of the kite against a gust will be exhibited. Figures 11 and 12 represent the most important variables. Initial conditions are selected in a equilibrium state with a constant wind ($W_0$ = 7 ms$^{-1}$ and δ = 55º). After 30 seconds, the gust appears and the wind velocity grows between 7ms$^{-1}$ and 7·5ms$^{-1}$. It can be seen (Fig. 12) that if the control system works the flight altitude keeps constant. However, if the system is without control the kite climbs to reach 96m. The control system detects a wind velocity rise and calculates the new δ that is necessary to keep the altitude. The consequence is that δ must be reduced. The new bridle's geometry makes the kite fly with a lower pitch angle. That can be explained taking into account that if the flight altitude is constant, aerodynamic forces must be constant too. When the wind velocity is greater, the kite produces the same normal force as if the attack angle is lower and therefore the pitch angle.

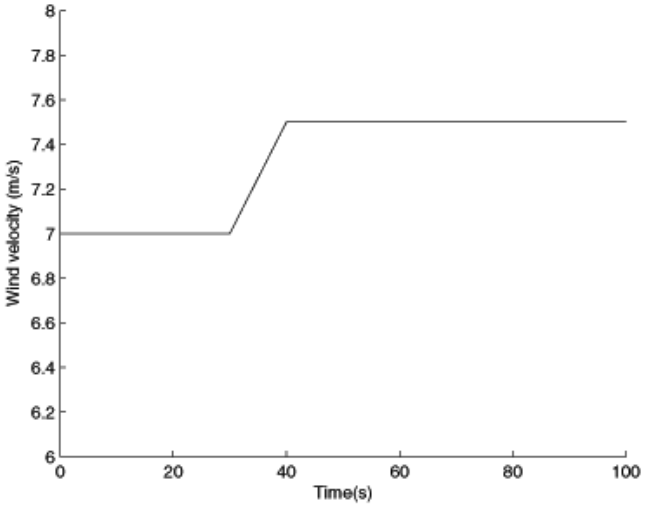


Figure 11. Wind velocity evolution.

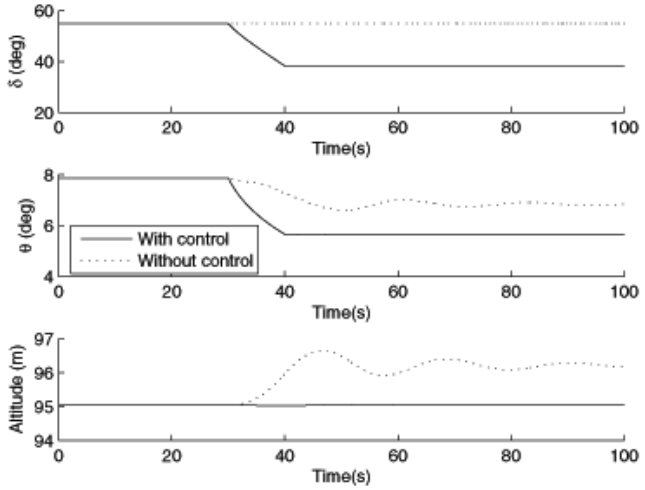


Figure 12. Behaviour of the kite against a gust.

The system control reveals how to act against a gust. However it must be said that the control became saturated with only a gust of 0·5ms$^{-1}$. In this situation the control parameter δ may change between 55º and 38·5º.

## 7.0 CONCLUSIONS

- A model with two degrees of freedom to simulate the dynamics of a single-line kite has been presented. If the union between the bridle and the principal line is ideal (without dissipation) Lagrangian formulation has some advantages. In particular the tension force disappears in the equations and a system of four ordinary equations can be obtained.
- The equilibrium state of the kite can be studied in an easy way. Two decoupled equations give both the pitch angle and the azimuth angle Γ. They depend only on three parameters: δ, σ and $\beta C_N$ and the results agree with Ref. 5. The system could present three equilibrium states but only the low angle of attack state is useful.
- Stability of such state is analysed with linear theory. Using this model the kite has two eigenmodes: pitch mode and pendulum mode that are in agree with J. DeLaurier's aerostats experiments. The stability of the system in the parametric plane δ – $W_0$ is calculated numerically. A line separates the parametric domain where the wind velocity is too low to support the kite. A region of instability appears when δ is above 55º. The system seems to be stable in a wide range of situations.
- The equilibrium state with low angle of attack changes its stability though a Hopf bifurcation. This bifurcation is supercritical when the wind velocity is not too high but strong winds make it subcritical. On the other hand, periodic branches are sometimes finished because the kite stalls or flies over Γ = 90. As a consequence, stable periodic orbits only exist in a small parametric domain in the plane δ – $W_0$.
- Stable periodic orbits could be harmful in some kite applications like aerial photography. Choosing an adequate geometry of the bridle and using Fig. 8 this kind of orbit can be avoided.
- Non-stationary wind conditions (gusts) change the flight altitude. Using an electric motor the geometry of the bridle can be changed and the kite can be controlled. The open loop control system works successfully when the wind velocity does not change too much. However it can be saturated if the gust is strong. Using a closed loop control law and by using two variables of control (*r* and δ) this problem can be solved and would also make the control more robust.
- The control system can make the kite fly with an optimum lift/drag ratio as proposed by K. Alexander and J. Stevenson improving the performances of a high altitude kite. However the weight of the kite will be increased by the mechanism and the engine, and the global impact above the system must be considered.

## ACKNOWLEDGMENTS

This work was partially supported by Ministerio de Ciencia y Tecnología of Spain, under Grant No. ESP2004-01511. The author thanks J. Pelaez for fruitful discussions and M. Romero for the thoroughly revision of the manuscript.

## REFERENCES

1. GLAUERT, H. The stability of a body towed by a light wire, *RM*, 1930, **1312**, Aeronautical Research Council, UK.
2. BAIRSTOW, L., RELF, E.F. and JONES, R. The stability of kite ballons: mathematical investigation, *RM*, December 1915, **208**, Aeronautical Research Council, UK.
3. BRYANT, L.W., BROWN, W.S. and SWEETING, N.E. Collected research on the stability of kites and towed gliders, *RM*, February 1942, **2303**, Aeronautical Research Council, National Physical Lab, Teddington Middlesex, UK.
4. ADOMAITIS, R.A. Kites and bifurcation theory, *SIAM Review*, September 1989, **31**, (3), pp 478-483.
5. ALEXANDER, K. and STEVENSON, J. Kite equilibrium and bridle length, *Aeronaut J*, September 2001, pp 535-541.
6. VELDMAN, S., BERSEE, H., VERMEEREN, C. and BERGSMA, O. Conceptual design of a high altitude kite, 2002, 43rd AIAA/ASME/ASCE/AHS/ASC Structures, Structural Dynamics, and Materials Conference, Denver, Colorado, 22-25 April, 2002.
7. DIEHL, M., MAGNI, L. and DE NICOLAO, G. Efficient NMPC of unstable periodic systems using approximate infinite horizon closed loop costing, *Annual Review in Control*, 2004, **28**, pp 37-45.
8. DELAURIER, J.D. Influence of ballonet motions on the longitudinal stability of tethered aerostats, *J Aircr*, May 1980, **17**, (5), pp 305-312.
9. Fluid forces and moments on flat plates, September 1970, ESDU International, Engineering Science Data Unit 70015.
10. DOEDEL, E.J., CHAMPMEYS, A.R., FAIRGRIEVE, T.F., KUZNETSOV, Y., SANSTEDE, B., WANG, X.J. AUTO 97: Continuation and bifurcation software for ordinary differential equations, 1997, pub/doedel/auto at ftp.cs.concordia.ca.
11. ERMENTROUT, B. XPPAUT, Dynamical systems software with continuation and bifurcation capabilities, 2000, /pub/bardware at ftp.math.pit.edu.